Hindawi
Advances in Civil Engineering
Volume 2024, Article ID 3884586, 19 pages
https://doi.org/10.1155/2024/3884586

Research Article

Stability Evaluation of the Goaf Based on Combination Weighting and Cloud Model

Linning Guo[1,2] **Kepeng Hou**[1,2] **Huafen Sun**[1,2] **and Yong Yang**[1,2]

[1]*Department of Resource Development Engineering, Kunming University of Science and Technology, Kunming 650000, China*
[2]*Yunnan Key Laboratory of Sino-German Blue Mining and Utilization of Special Underground Space, Kunming University of Science and Technology, Kunming 650000, China*

Correspondence should be addressed to Kepeng Hou; 11301046@kust.edu.cn and Huafen Sun; 20140091@kust.edu.cn

Received 13 September 2023; Revised 12 November 2023; Accepted 5 December 2023; Published 29 February 2024

Academic Editor: Tianshou Ma

Goaf has become one of the most significant sources of hazard affecting the safety of metal and nonmetal mines. Evaluation of goaf stability is of paramount importance for mine safety production. First, 13 indices such as rock mass structure, geological structure, and goaf volume are selected based on engineering experience and literature review to assess the stability of goaf. These indices are classified according to the characteristics of each factor, and a stability evaluation system for underground mine goaf is constructed. Second, the analytic hierarchy process method based on group decision theory is utilized to calculate the subjective weight of each index. Additionally, the CRITIC method is used to calculate the objective weight of each index. Finally, game theory is used to combine the subjective and objective weights, thereby improving the accuracy of the index weight. The stability grade of the goaf is calculated using the normal cloud model. The FLAC3D numerical simulation is used to analyze the stability of the goaf and verify the accuracy of the model. The abovementioned model is utilized for assessing the stability of the goaf in the Duimenshan mine section. The results indicate that 90% of the goaf area is in a stable or relatively stable condition, while the remaining 10% is unstable. The evaluation outcomes were compared with FLAC3D numerical simulations, highlighting a scientific and reliable method with an accuracy rate of 90%.

1. Introduction

China has become a leading mining nation for both metal and nonmetallic mineral resources globally, and as such, their development and utilization have become an imperative for China's social and economic progress. Based on limited data, the open-stope mining method represents around 60% of all metal and nonmetal underground mining conducted in China. Data on safety accidents in China's metal and nonmetal mines from 2001 to 2014 show that 65 incidents of collapse and roof fall occurred in goafs, leading to the death of 252 people, accounting for 47.1% and 47.4% of the total number of accidents, respectively. Seventy percent of the goaf at China's metal and nonmetallic mines have varying degrees of safety hazards, making them one of the main sources of risk to the safe production of such mines. As such, assessing the stability of goafs is a crucial aspect of ensuring mine safety protocols [1].

A significant amount of research has been conducted by scholars on evaluating the stability of goaf. For instance, Shang et al. [2] employed FLAC3D to simulate the stability of the overlying rock mass in the goaf. They found that tensile failure dominated the upper part of the middle goaf, while tensile shear failure dominated the upper rock masses on both sides. A 19-channel microseismic monitoring system was constructed by Liu et al. [3] to monitor the surrounding rock of the goaf hanging wall continuously. The microseismic activity is used to analyze the stability of the mine goaf. Jia et al. [4] proposed the ITOPSIS and point safety factors comprehensive analysis method, which analyzes the local stability of goaf. Zhao et al. [5] proposed a fuzzy random reliability analysis method that is based on block theory and fuzzy measure theory in fuzzy analysis to evaluate block stability. Using this method, they analyzed the stability of surrounding rock blocks in goaf roof. Hu et al. [6] employed the analytic hierarchy process (AHP) to analyze the weight of

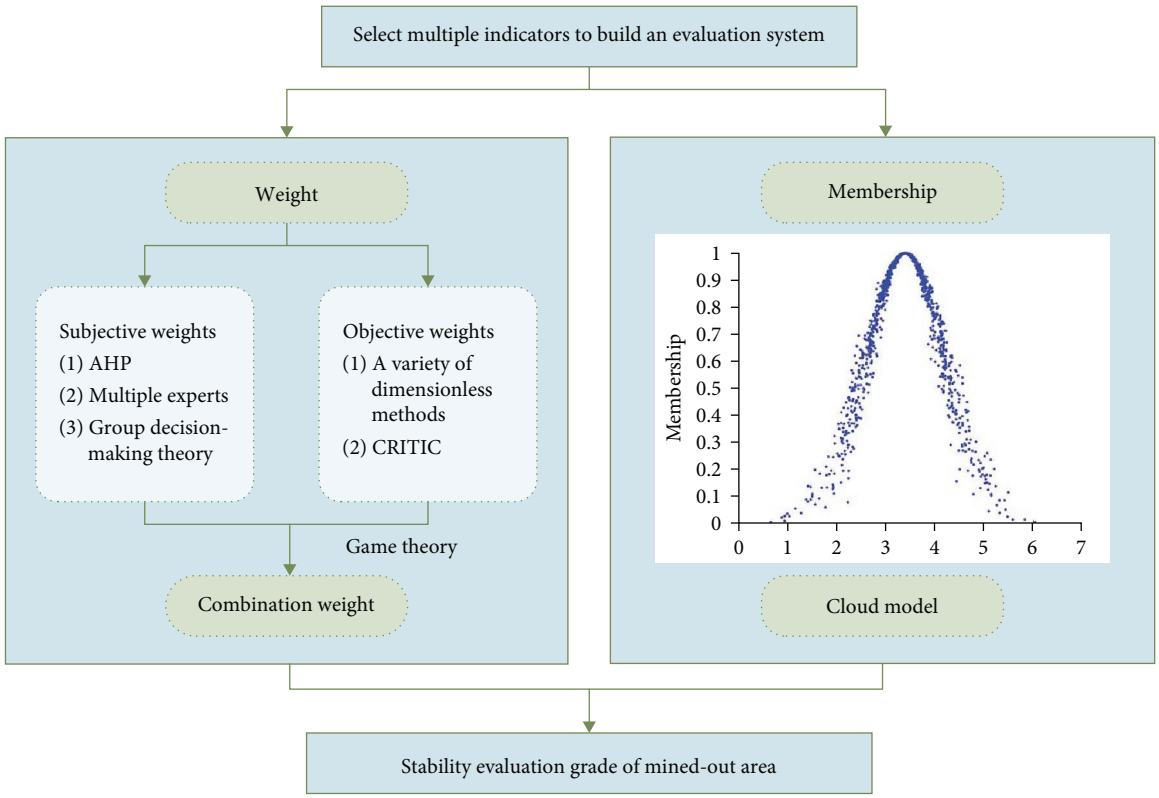

Figure 1: Flowchart of stability grade evaluation of goaf area.

factors. They developed a stability analysis model of group goaf based on D-S evidence theory's multisource information fusion. He et al. [7] created the goaf stability model by using the double-layer fuzzy comprehensive evaluation method. An improved TrAdaBoost algorithm based on transfer learning theory was proposed by Qin et al. [8] for predicting goaf stability. Wang et al. [9] established a stability evaluation model for the construction site above the goaf based on variable weight theory and regret theory. Luo et al. [10] developed a method for evaluating the stability of point columns in goaf using the weighted distance approximation of hesitant fuzzy genetic algorithm (GA-WDBA). Yuan et al. [11] investigated principal component analysis and differential evolution (DE) algorithm and employed multiclassification support vector machine to classify goaf risk.

Although the previous research methods have yielded favorable results in investigating goaf stability, the numerical simulation and online monitoring data entail significant complexity and effort. Evaluating the stability of goaf involves a nonlinear problem, with inherent randomness and fuzziness in the evaluation index. Yet, most evaluation models employ a relatively simple method to calculate the index weight, with some models failing to consider the randomness of evaluation indexes.

To address the aforementioned issues, this paper utilizes an improved AHP based on group decision theory to determine the subjective weight of the index. Additionally, the objective weight of the index is calculated using the CRITIC method, and game theory is leveraged to merge the two weights to enhance the accuracy of the index weight. Based on these findings, the cloud model estimates the stability of the goaf, standardizes the randomness of the evaluation index, and enhances the accuracy of the evaluation results.

2. Materials and Methods

This paper establishes an evaluation index system and employs the improved AHP, CRITIC method, and game theory to calculate the combined weight. Subsequently, the stability level of the goaf is evaluated using the cloud model. Figure 1 illustrates the calculation process.

2.1. Construction of Evaluation Index System. Goaf instability is associated with geological factors, goaf geometric parameters, hydrological factors, and engineering geological conditions. Existing goaf disasters, and research on underground engineering stability, 13 indicators were selected to evaluate goaf stability. These include rock mass structure, geological structure, rock mass quality, goaf volume, maximum exposed area, height, span, burial depth, ore body dip angle, exposure time, adjacent goaf and follow-up mining disturbance, and groundwater situation, following scientific and comprehensive index selection principles [12–18]. The resulting goaf stability evaluation system, shown in Figure 2, is specific to metal mine mountains.

According to references, the stability of goafs in metal underground mines is divided into four grades: I, II, III, and IV. Level II indicates poor stability of goafs; Level III indicates that goafs are more stable; and Level IV indicates

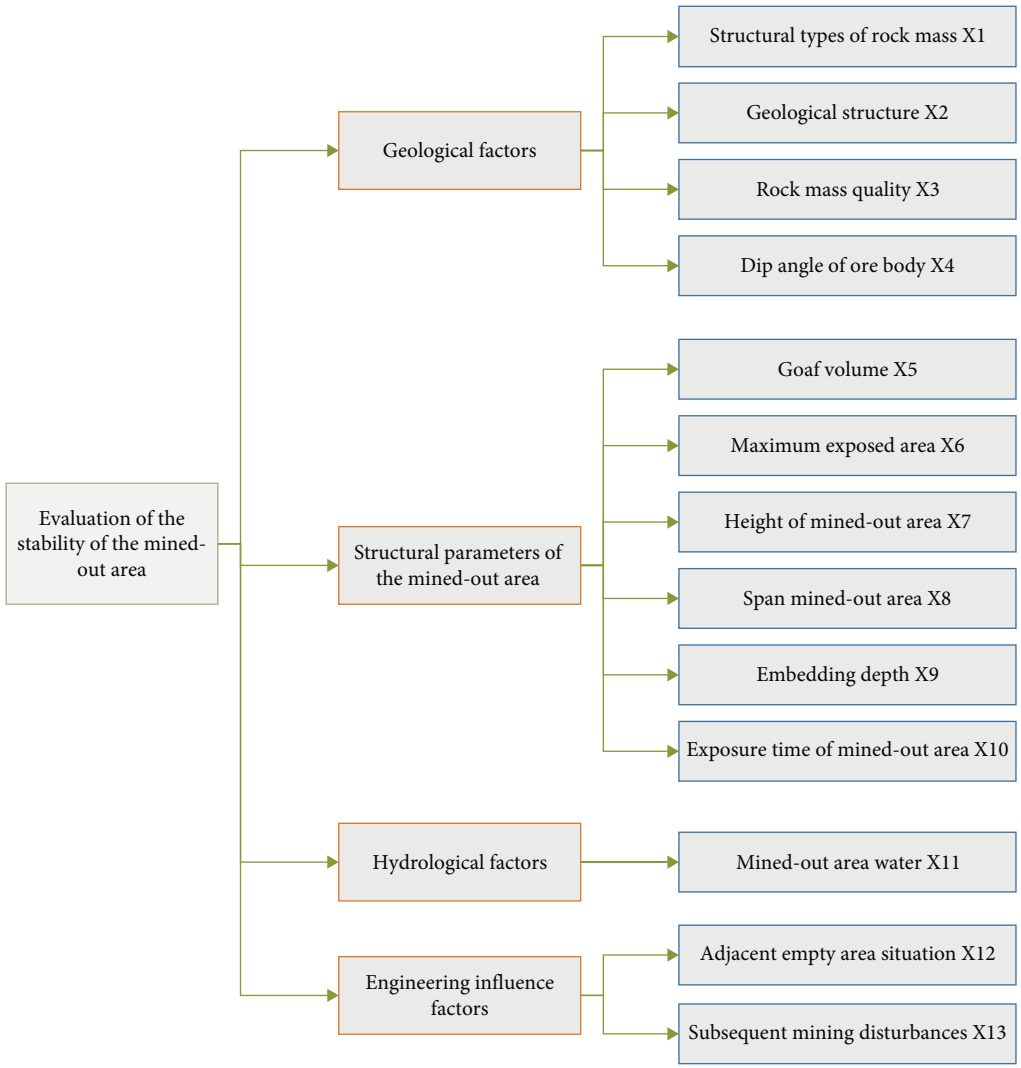

Figure 2: Evaluation system of goaf stability.

greater goaf stability [19–22]. Tables 1 and 2 show the corresponding standards of indicators for the different goaf stability levels.

2.2. Subjective Weighting of AHP Based on Group Decision Theory. The AHP is a systematic method of analysis that combines qualitative and quantitative analysis. It compares the indicators at all levels pairwise to determine their weights [23, 24]. Under normal circumstances, decisions are made by several members. In data processing, the traditional method involves obtaining the average value of the evaluation scale from decision makers and then calculating the weight. However, this method is unable to test the consistency of a judgment matrix given by a single decision maker, and the evaluation results may not meet consistency requirements. Different decision makers have varying levels of cognitive ability, which means that the above method does not accurately reflect evaluation results that differ greatly. A comprehensive analysis suggests that averaging evaluation matrices of multiple decision makers is imprecise.

To ensure index weight rationality and accuracy, a group consistency test must be conducted on the evaluations of multiple decision makers. Decision makers with marked inconsistency with group opinions should be identified, and measures taken to obtain reasonable weights. Group decision making is a method for considering convergence of decisions made by multiple decision makers [25–27]. Therefore, weights are calculated using the coupled AHP and group decision theory. The following steps are involved in the calculation:

(1) Weight vector of evaluation criteria for a single decision maker.
   (i) Construct a matrix to assess the criteria.

The evaluation group was composed of m decision makers, and the evaluation weight of each decision-maker on n indexes was obtained by using AHP. The 1–9 scale method is used to compare each index in pairwise, and the judgment matrix is obtained A_k:

Table 1: Qualitative grading and assignment of the stability evaluation of the goaf.

Factors	Class			
	Class I	Class II	Class III	Class IV
Assign a value	1	2	3	4
Structural types of rock mass X1	Loose surrounding rock	The surrounding rock is broken showing small pieces	The surrounding rock is a laminated structure	Surrounding rock integrity
Geological structure X2	Fault penetration through the surrounding rock	Located in the lower plate of the fault and the top plate of the empty area is connected to the fault	The roof located in the footwall of the fault is far away from the fault	Located on the upper plate of the fault
Mined-out area water X11	The surrounding rocks in the goaf have seepage for a long time, and the surrounding rocks are affected by the water body	There is seepage in the rainy season in the goaf, and the surrounding rock is affected by the water body	Water traces are visible in the surrounding rocks of the goaf, and the surrounding rocks are less affected by the water body	No seepage and no water traces in the surrounding rock of the goaf, no water body around the surrounding rock
Adjacent empty area situation X12	The surrounding goaf is connected and densely forms a large connected area	The number of goafs in the vicinity of the goaf is high, the area is not large, and they are close to each other	The goaf near the goaf is small, not large, and scattered	Independent goaf
Subsequent mining disturbances X13	The empty area is located in the subsequent proposed goaf	The empty area is located in the proposed goaf mining larger impact range	The vacant area is located in the less influential area of the proposed goaf	The vacant area is located outside the area of influence of the proposed goaf

Table 2: Grading criteria of quantitative indicators for the evaluation of the stability of the goaf.

Factors	Class			
	Class I	Class II	Class III	Class IV
Rock mass quality X3 (%)	<50	(50, 70)	(70, 90)	≥90
Dip angle of ore body X4 (degree)	<3	(3, 30)	(30, 50)	≥50
Goaf volume X5 (10^3, m^3)	≥81	(24, 81)	(6.4, 24)	<6.4
Maximum exposed area X6 (m^2)	≥2,700	(1,200, 2,700)	(800, 1,200)	<800
Height of mined-out area X7 (m)	≥30	(20, 30)	(8, 20)	<8
Span of mined-out area X8 (m)	≥120	(80, 120)	(40, 80)	<40
Embedding depth X9 (m)	≥600	(450, 600)	(300, 450)	<300
Exposure time of goaf X10 (a)	≥20	(10, 20)	(6, 10)	<6

Table 3: RI values.

n	1	2	3	4	5	6	7	8	9	10
RI	0.00	0.00	0.58	0.90	1.12	1.24	1.32	1.41	1.45	1.49

$$A_p = \{a_{ij}\}_{n\times n}. \tag{1}$$

(ii) Calculate the weight of evaluation indicators.

First, each column of the judgment matrix is normalized to get a vector V, and then find the sum of the rows in the vector V, computed vector V_i. Finally, each element in the vector V_i is normalized to get the weight vector W_k:

$$\begin{aligned} V &= \begin{bmatrix} a_{11}/\sum_{i=1}^{n} a_{i1} & a_{12}/\sum_{i=1}^{n} a_{i2} & \cdots & a_{1n}/\sum_{i=1}^{n} a_{in} \\ a_{21}/\sum_{i=1}^{n} a_{i1} & a_{22}/\sum_{i=1}^{n} a_{i2} & \cdots & a_{2n}/\sum_{i=1}^{n} a_{in} \\ \vdots & \vdots & \ddots & \vdots \\ a_{n1}/\sum_{i=1}^{n} a_{i1} & a_{n2}/\sum_{i=1}^{n} a_{in} & \cdots & a_{nn}/\sum_{i=1}^{n} a_{in} \end{bmatrix} \rightarrow \\ V_i &= \begin{bmatrix} a_{11}/\sum_{i=1}^{n} a_{i1} + a_{12}/\sum_{i=1}^{n} a_{i2} + \cdots + a_{1n}/\sum_{i=1}^{n} a_{in} \\ a_{21}/\sum_{i=1}^{n} a_{i1} + a_{22}/\sum_{i=1}^{n} a_{i2} + \cdots + a_{2n}/\sum_{i=1}^{n} a_{in} \\ \vdots \\ a_{n1}/\sum_{i=1}^{n} a_{i1} + a_{n2}/\sum_{i=1}^{n} a_{in} + \cdots + a_{nn}/\sum_{i=1}^{n} a_{in} \end{bmatrix} = \begin{bmatrix} v_1 \\ v_2 \\ \vdots \\ v_n \end{bmatrix} \rightarrow \\ W_k &= \begin{bmatrix} v_1/\sum_{i=1}^{n} v_i & v_2/\sum_{i=1}^{n} v_i & \cdots & v_n/\sum_{i=1}^{n} v_i \end{bmatrix}^T \end{aligned}. \tag{2}$$

(iii) Consistency check.

Calculate the maximum characteristic root of the judgment matrix $\lambda_{\max}$, calculate consistency metrics CI, found the corresponding average random consistency RI (Table 3), and calculate the consistency ratio CR. When CR < 0.10, we believe that the judgment matrix meets the consistency requirements, otherwise we need to make appropriate adjustments to the judgment matrix until it passes the consistency test:

$$\lambda_{\max} = \sum_{i=1}^{n} \frac{(A_k \cdot W_k)}{nW_k}, \tag{3}$$

$$\mathrm{CI} = \frac{\lambda_{\max} - n}{n-1}, \tag{4}$$

$$\mathrm{CR} = \frac{\mathrm{CI}}{\mathrm{RI}}. \tag{5}$$

(2) Group consistency algorithm.

(i) The cosine of the vector angle of the indicator weights of the two decision makers $p$and$q$ are calculated to determine whether there is strong consistency between them. If $(\cos\theta)_{p,q} \geq \alpha$, then there are strong consistency between the two decision makers, and if $(\cos\theta)_{p,q} \leq \beta$, then there is strong inconsistency between the two decision makers:

$$(\cos\theta)_{p,q} = \frac{w_p \cdot w_q}{\|w_p\| \times \|w_q\|}. \tag{6}$$

(ii) Calculate the group strong consistency index GAI and group strong inconsistency index GDI of decision makers based on the cosine of the angle between the weight vectors of decision makers' indicators:

$$\mathrm{GAI} = \frac{\sum_{p\in M}\sum_{p<q} 2Z(p,q)}{m(m-1)}, Z(p,q) = \begin{cases} 1 & (\cos\theta)_{p,q} \geq \alpha \\ 0 & (\cos\theta)_{p,q} < \alpha \end{cases}. \tag{7}$$

$$\mathrm{GDI} = \frac{\sum_{p\in M}\sum_{p<q} 2V(p,q)}{m(m-1)}, V(p,q) = \begin{cases} 1 & (\cos\theta)_{p,q} \leq \beta \\ 0 & (\cos\theta)_{p,q} > \beta \end{cases}. \tag{8}$$

(iii) Calculation of individual strong consistency and individual strong inconsistency indicators for decision makers:

Table 4: Commonly used dimensionless methods.

Serial no.	Dimensionless method	Function expressions
Method 1	Range transformation method (MMS)	$x_{ij}^{*}=\frac{x_{ij}-\min(x_j)}{\max(x_j)-\min(x_j)}$
Method 2	Standardization method (S)	$x_{ij}^{*}=\frac{x_{ij}-\frac{1}{m}\sum_{i=1}^{m}x_{ij}}{\sqrt{\frac{1}{m-1}\sum_{i=1}^{m}(x_{ij}-\overline{x_j})}}$
Method 3	Averaging method (MC)	$x_{ij}^{*}=\frac{x_{ij}}{\frac{1}{m}\sum_{i=1}^{m}x_{ij}}$
Method 4	Differentiated polarization transformation method (MMS, NMMS)	$MMS\,x_{ij}^{*}=\frac{x_{ij}-\min(x_j)}{\max(x_j)-\min(x_j)}$ $NMMS\,x_{ij}^{*}=\frac{\max(x_j)-x_{ij}}{\max(x_j)-\min(x_j)}$
Method 5	Natural logarithm method (ln)	$x_{ij}^{*}=\ln(x_{ij})$
Method 6	Logarithm with base 10 (log10)	$x_{ij}^{*}=\log_{10}(x_{ij})$
Method 7	Summation normalization (SN)	$x_{ij}^{*}=\frac{x_{ij}}{\sum_{i=1}^{m}x_{ij}}$
Method 8	Square and summation normalization (SSN)	$x_{ij}^{*}=\frac{x_{ij}}{\sqrt{\sum_{i=1}^{m}x_{ij}^{2}}}$

$$\mathrm{IAI}_p=\frac{\sum_{p\in M,p\neq q}Z(p,q)}{(m-1)},\ Z(p,q)=\begin{cases}1 & (\cos\theta)_{p,q}\geq\alpha\\ 0 & (\cos\theta)_{p,q}<\alpha\end{cases}. \tag{9}$$

$$\mathrm{IDI}_p=\frac{\sum_{p\in M,p\neq q}V(p,q)}{(m-1)},\ V(p,q)=\begin{cases}1 & (\cos\theta)_{p,q}\leq\beta\\ 0 & (\cos\theta)_{p,q}>\beta\end{cases}. \tag{10}$$

(iv) The reliability λ_p' of the indicator weights of decision maker p is calculated and normalized to obtain the m decision maker weight vector:

$$\lambda_p'=\frac{\mathrm{IAI}_p\times\left(1-\mathrm{IDI}_p\right)}{\mathrm{GAI}\times(1-\mathrm{GDI})}. \tag{11}$$

$$\lambda_p=\frac{\lambda_p'}{\sum_{p=1}^{m}\lambda_p'}. \tag{12}$$

(v) The indicator weight vector of each decision maker is multiplied with the decision maker weight vector and averaged to obtain the subjective weight vector:

$$W=\frac{\sum_{k=1}^{m}\sum_{p=1}^{m}W_k\cdot\lambda_p}{m}. \tag{13}$$

2.3. Objective Empowerment Based on CRITIC Method. The CRITIC weighting method is an objective approach that considers the strength of contrast and conflict between indicators to derive weightings [28, 29]. The calculation follows specific steps:

(1) Dimensionless indexing.

The initial values of evaluation indexes are processed using the following dimensionless methods, as shown in Table 4, combined with the characteristics of 13 evaluation indexes. After conducting comparative research, we have selected the methods that fully reflect the contrasting strength and conflict of indexes.

(2) Equations (14) and (15) were utilized to compute the relative intensity of indicators:

$$s_j=\sqrt{\frac{1}{m-1}\sum_{i=1}^{m}\left(x_{ij}-\overline{x_j}\right)}, \tag{14}$$

$$\overline{x_j}=\frac{1}{m}\sum_{i=1}^{m}x_{ij}. \tag{15}$$

(3) Equations (16) and (17) were used to calculate the conflicting nature of the indicators:

$$\eta_j=\sum_{i=1}^{n}\left(1-r_{ij}\right), \tag{16}$$

$$r_{ij}=\frac{\sum_{j,k=1}^{n}\left(x_{ij}-\overline{x_j}\right)\times\left(x_{ik}-\overline{x_k}\right)}{\sqrt{\sum_{j=1}^{n}\left(x_{ij}-\overline{x_j}\right)^2\times\sum_{k=1}^{n}\left(x_{ik}-\overline{x_k}\right)^2}}. \tag{17}$$

(4) The amount of index information was calculated by using Equation (18):

$$C_j=s_j\times\eta_j. \tag{18}$$

(5) To obtain objective weights, the indicator information is normalized:

$$W_j=\frac{C_j}{\sum_{j=1}^{n}C_j}. \tag{19}$$

2.4. Game Theory-Based Portfolio Assignment. The problem of determining optimal combination weights for indicators is resolved by using assembly game theory. The method aims to establish equilibrium or compromise between potential weights by reducing deviation between the combination weights and the

weights determined through various approaches. This enhances the scientific and reliable nature of the evaluation index [30, 31].

The weight vector of the indicator obtained through the hierarchical analysis based on group decision theory is denoted by $\vec{W}_1^T$, and the weight vector of the indicator calculated using CRITIC is denoted by $\vec{W}_2^T$. Let $\vec{W}$ represents the linear combination of weight vectors $\vec{W}_1^T$ and $\vec{W}_2^T$ with α_P as the combination coefficient, i.e.:

$$\vec{W} = \sum_{P=1}^{2} \alpha_P \vec{W}_P^T. \tag{20}$$

$\vec{W}$ is determined by minimizing the deviation of W from $\vec{W}_1^T$ and $\vec{W}_2^T$. The countermeasure model is obtained by the following equation:

$$\min \left\| \sum_{P=1}^{2} \alpha_P \vec{W}_P^T - \vec{W}_l^T \right\|. \tag{21}$$

Solving Equation (19) leads to α_P, which is then normalized. The combined weight vector can be obtained as follows:

$$\vec{W}^* = \sum_{P=1}^{2} \alpha_P{}^* \vec{W}_P^T. \tag{22}$$

2.5. Cloud Model Evaluation Method Based on Combination Assignment. The cloud model can serve as an uncertainty model for converting qualitative to quantitative measurements by synthesizing the fuzziness and randomness of evaluation indexes and thus enabling the natural conversion between qualitative language and quantitative values. The cloud model relies on the characteristics of expectation (*Ex*), entropy (*En*), and super entropy (*He*) to generate cloud drops, which can contribute to various models [32, 33]. The following expressions represent the cloud characteristics parameters of the evaluation level:

$$\begin{cases} E_{xi} = \dfrac{x_{\max}^i + x_{\min}^i}{2} \\ E_{ni} = \dfrac{x_{\max}^i - x_{\min}^i}{2\sqrt{2\ln 2}}, \\ E_{ei} = k \end{cases} \tag{23}$$

where $x_{\max}^i$ and $x_{\min}^i$ are the maximum and minimum values of different index evaluation levels. k is a constant, generally taking values between 0.001 and 0.1. In this paper, according to the fuzzy degree of the rubric itself and with reference to previous literature, the value of k is 0.01.

Specific algorithms are required to implement the cloud model. The forward cloud generator is selected in this paper to quantify qualitative concepts and assess the stability of the goaf. Figure 3 demonstrates the calculation steps.

The already obtained combined weight vector W^* is point multiplied by the affiliation degree $\mu(x_i)$ of the n evaluation indexes of each goaf to obtain the comprehensive determination degree D_k of the stability of the goaf, and the stability level of the goaf is determined according to $\max(D_k)$:

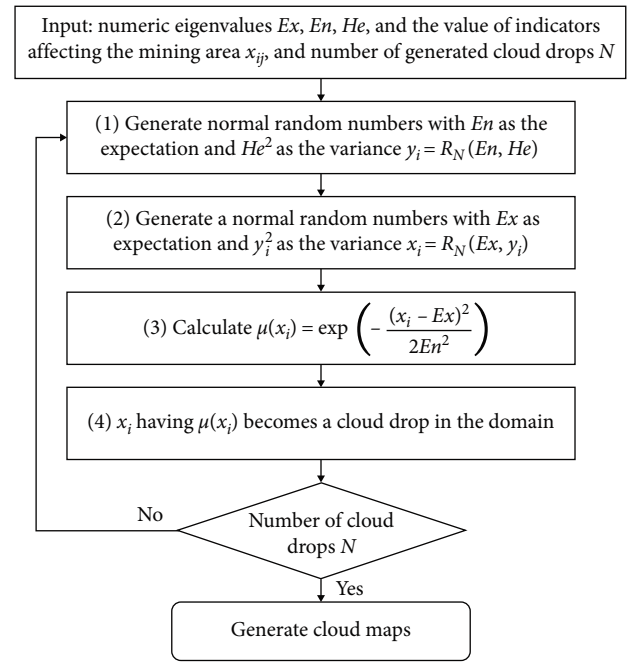

Figure 3: Positive cloud generator.

$$D_k = \sum_{i=1}^{n} \mu(x_i) \cdot W_i. \tag{24}$$

3. Results and Discussion

In order to verify the feasibility and rationality of the goaf stability evaluation model, the established model was used to evaluate the stability of 151 goafs in Duimenshan mine section, and FLAC3D software was used to analyze the stability of Duimenshan goaf. The calculation results of the two methods were compared to further verify the rationality of the goaf stability evaluation model.

3.1. Goaf Investigation. In the Duimenshan section of the Bainiuchang Mine, 20 middle sections have been mined since 2003. The rock conditions surrounding the goaf are favorable. The survey primarily relies on 3D laser scanning, complemented by geophysical prospecting and field surveys. The middle section of the Duimenshan section has 151 goafs within the 1,830–1,500 m range. Table 5 displays the survey data of the goaf.

3.2. Calculation of Goaf Stability Evaluation Model

3.2.1. Calculation of Combination Weights

(1) Calculation of the subjective weights of decision makers was achieved using the AHP of group decision theory.

The panel of decision makers (Di) consisted of 10 experts, academics, and technicians in the field of mining and safety. Back-to-back comparisons of the 13 indicators affecting mine stability were conducted using hierarchical analysis. The judgment matrices of the 10 decision makers are presented on a nine-level scale (Tables S1–S10). Based on the

Table 5: Survey data of goaf.

No.	X1	X2	X3 (%)	X4 (degree)	X5 (m^3)	X6 (m^2)	X7 (m)	X8 (m)	X9 (m)	X10 (a)	X11	X12	X13
1525-1	4	4	61.11	40	169	85	7	9	508	10	4	4	4
1525-2	4	4	61.11	32	710	304	13	19	508	10	2	4	4
1525-3	4	4	61.11	53	237	68	8	15	495	10	4	4	4
1525-4	4	3	61.11	45	1536	768	18	24	529	9	3	3	3
⋮	⋮	⋮	⋮	⋮	⋮	⋮	⋮	⋮	⋮	⋮	⋮	⋮	⋮
1660-4	4	4	66.38	48	503	93	5	4	330	12	4	4	4
1660-5	4	4	66.38	39	702	180	4	5	355	12	4	4	4
1660-6	4	4	66.38	68	1751	318	6	12	365	13	4	4	4
⋮	⋮	⋮	⋮	⋮	⋮	⋮	⋮	⋮	⋮	⋮	⋮	⋮	⋮
1830-3	3	2	57.09	20	10,748	1,124	13	18	213	14	3	3	3
1830-4	3	2	57.09	16	6,091	1,406	4	24	243	14	3	3	3

Table 6: Weighting of evaluation indicators for decision makers.

	D1	D2	D3	D4	D5	D6	D7	D8	D9	D10
X1	0.0867	0.0956	0.0822	0.1190	0.0963	0.1111	0.1072	0.0902	0.0572	0.0731
X2	0.1030	0.1137	0.0977	0.0841	0.0963	0.0785	0.0901	0.1072	0.0753	0.0962
X3	0.0729	0.0956	0.0691	0.0595	0.0963	0.0467	0.0901	0.0758	0.0680	0.0615
X4	0.0433	0.0433	0.0411	0.0421	0.0963	0.0467	0.0758	0.0451	0.0366	0.0330
X5	0.0874	0.0697	0.0868	0.0890	0.0855	0.1131	0.0790	0.0678	0.0928	0.1045
X6	0.0874	0.0749	0.0868	0.0804	0.0740	0.1345	0.0790	0.0807	0.1027	0.1045
X7	0.0874	0.0829	0.0868	0.0804	0.0719	0.0673	0.0940	0.0678	0.0928	0.0878
X8	0.1237	0.0918	0.1032	0.0804	0.0880	0.0673	0.0664	0.0751	0.1221	0.1521
X9	0.0618	0.0403	0.0730	0.0804	0.0386	0.0673	0.0664	0.0678	0.0780	0.0472
X10	0.0437	0.0257	0.0434	0.0402	0.0273	0.0673	0.0470	0.0306	0.0419	0.0472
X11	0.0777	0.0871	0.0927	0.0732	0.0871	0.0830	0.0670	0.1209	0.0852	0.0670
X12	0.0624	0.0853	0.0549	0.0856	0.0853	0.0470	0.0690	0.1026	0.0590	0.0630
X13	0.0624	0.0569	0.0823	0.0856	0.0569	0.0704	0.0690	0.0684	0.0885	0.0630

Table 7: $(\cos\theta)_{p.q}$.

$(\cos\theta)_{p.q}$	D1	D2	D3	D4	D5	D6	D7	D8	D9	D10
D1	1.0000	0.9778	0.9922	0.9697	0.9600	0.9453	0.9656	0.9585	0.9820	0.9878
D2	0.9778	1.0000	0.9708	0.9622	0.9787	0.9143	0.9711	0.9798	0.9425	0.9465
D3	0.9922	0.9708	1.0000	0.9777	0.9535	0.9569	0.9694	0.9686	0.9882	0.9716
D4	0.9697	0.9622	0.9777	1.0000	0.9511	0.9594	0.9780	0.9676	0.9563	0.9390
D5	0.9600	0.9787	0.9535	0.9511	1.0000	0.9148	0.9780	0.9630	0.9266	0.9261
D6	0.9453	0.9143	0.9569	0.9594	0.9148	1.0000	0.9464	0.9236	0.9424	0.9308
D7	0.9656	0.9711	0.9694	0.9780	0.9780	0.9464	1.0000	0.9581	0.9420	0.9246
D8	0.9585	0.9798	0.9686	0.9676	0.9630	0.9236	0.9581	1.0000	0.9406	0.9182
D9	0.9820	0.9425	0.9882	0.9563	0.9266	0.9424	0.9420	0.9406	1.0000	0.9785
D10	0.9878	0.9465	0.9716	0.9390	0.9261	0.9308	0.9246	0.9182	0.9785	1.0000

judgment matrices of the 10 decision makers for the 13 indicators, the weights of the indicators for each of the 10 decision makers were calculated using Equations (1)–(5). The results are shown in Table 6.

The cosine of the angle of the indicator vector between the decision makers can be calculated using Equation (6). The results of this calculation are presented in Table 7

Here, the values of α and β are not given, and the effects of different values of α and β on λ_p and W are compared. Usually, $\alpha \geq 0.67$ and $\beta \leq 0.5$ [34], according to Equations (7)–(13), through a large number of trial calculations, it is found that when $\beta \leq 0.9$, $\mathrm{GDI} = 0$, $\mathrm{IDI}_p = 0$ are obtained and therefore, with $\beta = 0.9$ unchanged, varying the value of α, when $\alpha \leq 0.91$, the decision weight of each decision maker is equal, i.e., $\lambda_p' = 0.01$.

Table 8: λ_p values.

α	0.91	0.92	0.93	0.94	0.95
D1	0.1	0.1071	0.1184	0.1250	0.1379
D2	0.1	0.0952	0.1053	0.1111	0.1034
D3	0.1	0.1071	0.1184	0.1250	0.1552
D4	0.1	0.1071	0.1184	0.1111	0.1379
D5	0.1	0.0952	0.0789	0.0833	0.1034
D6	0.1	0.0833	0.0789	0.0694	0.0345
D7	0.1	0.1071	0.1053	0.1111	0.1034
D8	0.1	0.0952	0.0921	0.0972	0.1034
D9	0.1	0.1071	0.1053	0.1111	0.0690
D10	0.1	0.0952	0.0789	0.0556	0.0517

Table 9: W values.

α	0.91	0.92	0.93	0.94	0.95
X1	0.0918	0.0915	0.0919	0.0918	0.0929
X2	0.0942	0.0942	0.0944	0.0947	0.0960
X3	0.0736	0.0738	0.0737	0.0746	0.0755
X4	0.0503	0.0502	0.0494	0.0500	0.0509
X5	0.0876	0.0872	0.0868	0.0859	0.0848
X6	0.0905	0.0898	0.0893	0.0884	0.0857
X7	0.0819	0.0825	0.0827	0.0828	0.0826
X8	0.0970	0.0975	0.0971	0.0962	0.0960
X9	0.0621	0.0626	0.0633	0.0634	0.0631
X10	0.0414	0.0412	0.0412	0.0406	0.0395
X11	0.0841	0.0838	0.0839	0.0845	0.0848
X12	0.0714	0.0714	0.0714	0.0717	0.0733
X13	0.0703	0.0708	0.0712	0.0712	0.0710

When $\alpha = 0.91, 0.92, 0.93, 0.94,$ and 0.95, the variation of λ_p and W is calculated (results are shown in Table 8, Table 9, Figure 4, and Figure 5).

Figure 4 shows that the weight of decision makers D1, D3, D4, D6, and D10 is more affected by the change in value, indicating that these decision makers intersect with the other five and are more individual. Figure 5 shows that the change in value has less impact on the weight. This indicates that there is high group consistency in this evaluation. Therefore, the judging thresholds of $\alpha = 0.91$ and $\beta = 0.5$ were chosen, and the weights were calculated: $W_1 = (0.0918, 0.0942, 0.0736, 0.0503, 0.0876, 0.0905, 0.0819, 0.0970, 0.0621, 0.0414, 0.084, 0.0714, 0.0703)$.

(2) Objective weights of factors calculation using the CRITIC method.

The index values (Table 5) were dimensionally processed using the eight dimensionless methods from Table 4. The comparison intensity, conflict, information quantity, and weight of the 13 indexes were subsequently calculated using Equations (14)–(19). The comparison results are depicted in Figures 6–9.

Figures 6–9 illustrate that the standardization (S) method for index deprogramming fails to reflect contrast intensity

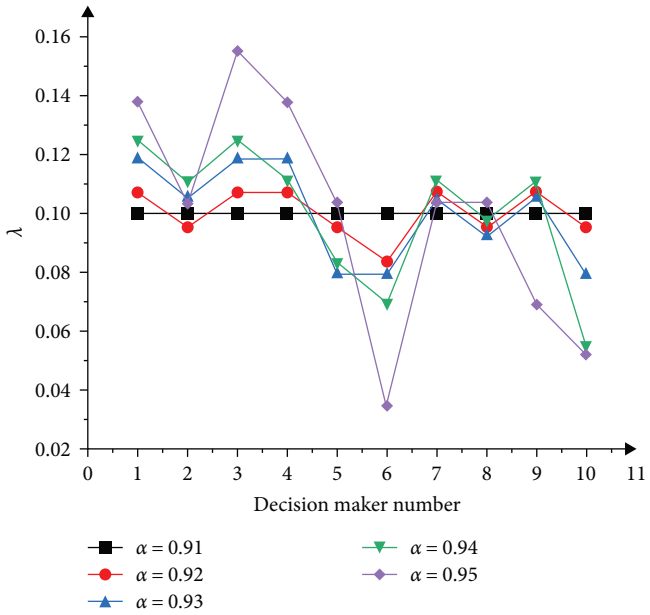

Figure 4: Variation of λ_p with α. The decision weights of 10 decision makers have been recorded using various evaluation criteria.

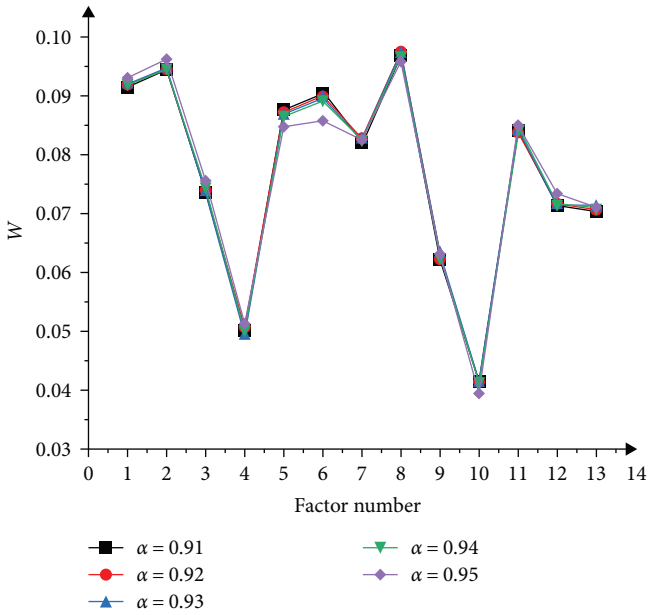

Figure 5: Variation of W with α. The evaluation criteria recorded subjective weights for 13 evaluation indexes.

and conflict between the indicators. Meanwhile, deprogramming using mean value, natural logarithm (ln), and log10 methods shows high contrast intensity between the indicators without clear conflicting nature. The normalization method (SN) and sum-of-squares normalization method yield weak contrast intensity between indicators and show no obvious conflict between the indicators. Although the contrast intensity between indicators of the extreme difference transformation method (MMS) and the differentiated extreme difference transformation method (MMS-NMMS) is medium, the

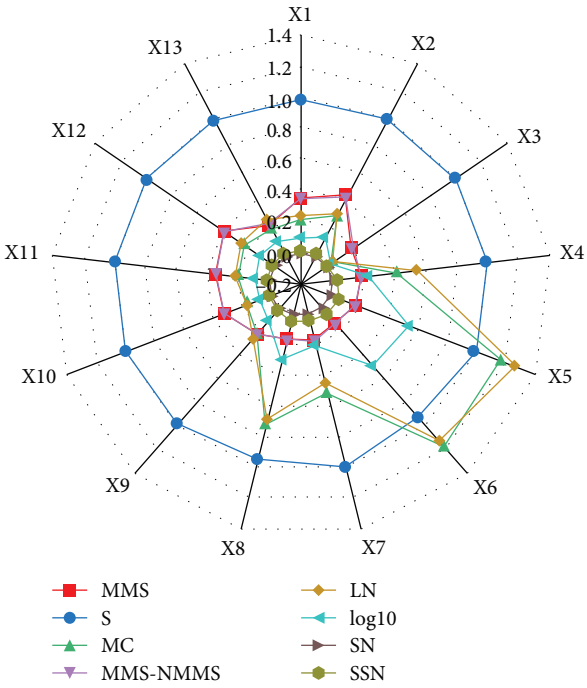

Figure 6: Comparative intensity of indicators.

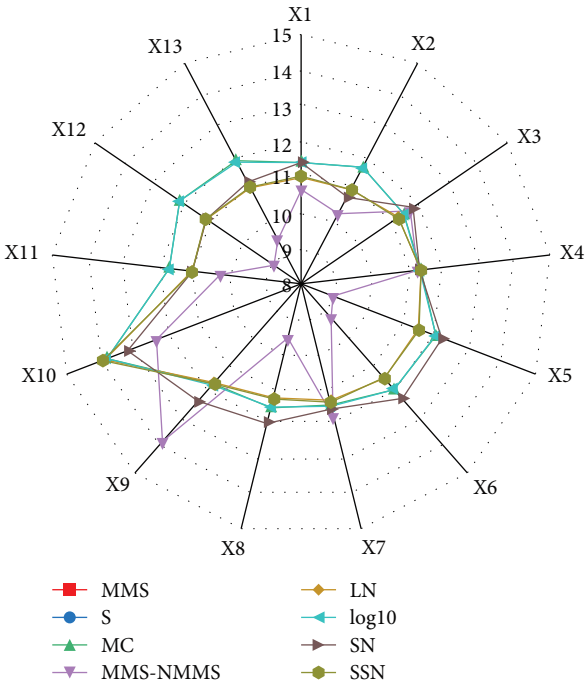

Figure 7: Conflicting indicators.

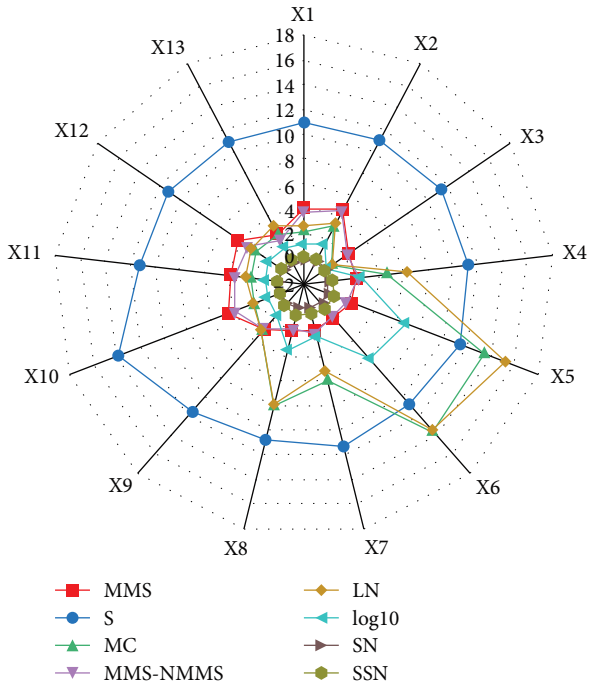

Figure 8: Indicator information volume.

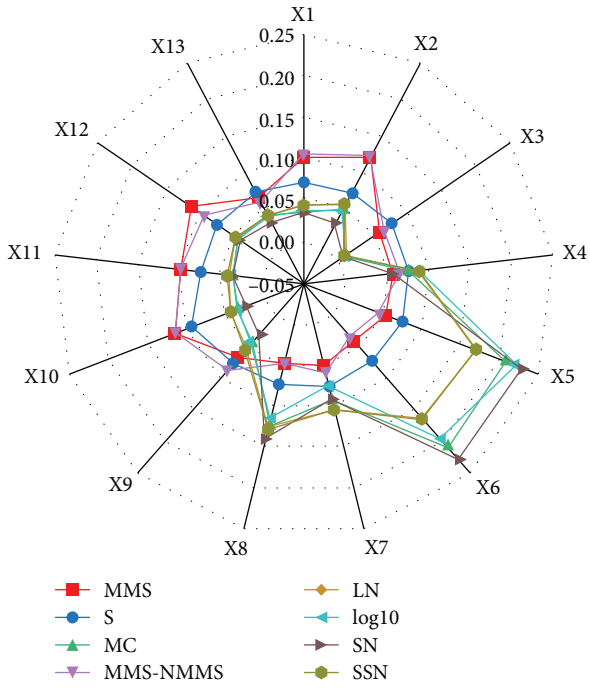

Figure 9: Weight of factors.

conflicting nature of the indicators is not obvious. Therefore, the differentiated extreme difference transformation method (MMS-NMMS) is selected for dequantizing the indicators and obtaining weight W2. The calculation results are illustrated in Table 10.

(3) Combination weighting based on game theory.

The above calculated W_1 and W_2 are calculated according to Equations (20) and (21) to obtain $\alpha_1 = 0.31$ and $\alpha_2 = 0.73$, normalized and reassigned weighting coefficients to obtain $\alpha_1^* = 0.30$ and $\alpha_2^* = 0.70$. The combined weights $W^* = (0.1025,\ 0.1157,\ 0.0696,\ 0.0598,\ 0.0583,\ 0.0515,\ 0.0651,\ 0.0599,\ 0.0794,\ 0.0896,\ 0.0941,\ 0.0893,\ 0.0641)$ are calculated according to Equation (22).

Table 10: Objective weights of the CRITIC method based on the MMS-NMMS.

Factors	Contrast intensity	Conflictual	Amount of information	Weights
X1	0.355	10.696	3.799	0.107
X2	0.432	10.258	4.432	0.1248
X3	0.207	11.653	2.41	0.0679
X4	0.2	11.317	2.265	0.0638
X5	0.183	8.896	1.63	0.0459
X6	0.135	9.193	1.238	0.0349
X7	0.175	11.769	2.056	0.0579
X8	0.165	9.5	1.565	0.0441
X9	0.222	13.849	3.081	0.0868
X10	0.316	12.363	3.907	0.1101
X11	0.339	10.301	3.495	0.0984
X12	0.384	8.973	3.442	0.0969
X13	0.231	9.473	2.184	0.0615

Table 11: Cloud characteristic parameters of each indicator under different levels.

Factors	Class I	Class II	Class III	Class IV
X1	(1, 0.425, 0.01)	(2, 0.425, 0.01)	(3, 0.425, 0.01)	(4, 0.425, 0.01)
X2	(1, 0.425, 0.01)	(2, 0.425, 0.01)	(3, 0.425, 0.01)	(4, 0.425, 0.01)
X3	(20, 16.987, 0.01)	(45, 4.247, 0.01)	(55, 4.247, 0.01)	(80, 16.987, 0.01)
X4	(1.5, 1.274, 0.01)	(16.5, 11.466, 0.01)	(40, 8.493, 0.01)	(70, 16.987, 0.01)
X5	(90,500, 8,068, 0.01)	(52,500, 24,205, 0.01)	(12,500, 7474, 0.01)	(3,200, 2,717, 0.01)
X6	(3,850, 977, 0.01)	(1,950, 637, 0.01)	(1,000, 170, 0.01)	(400, 340, 0.01)
X7	(45, 12.74, 0.01)	(25, 4.247, 0.01)	(14, 5.096, 0.01)	(4, 3.397, 0.01)
X8	(160, 33.973, 0.01)	(100, 16.987, 0.01)	(60, 16.987, 0.01)	(20, 16.987, 0.01)
X9	(900, 255, 0.01)	(500, 85, 0.01)	(300, 85, 0.01)	(100, 85, 0.01)
X10	(35, 12.74, 0.01)	(15, 4.247, 0.01)	(8, 1.699, 0.01)	(3, 2.548, 0.01)
X11	(1, 0.425, 0.01)	(2, 0.425, 0.01)	(3, 0.425, 0.01)	(4, 0.425, 0.01)
X12	(1, 0.425, 0.01)	(2, 0.425, 0.01)	(3, 0.425, 0.01)	(4, 0.425, 0.01)
X13	(1, 0.425, 0.01)	(2, 0.425, 0.01)	(3, 0.425, 0.01)	(4, 0.425, 0.01)

(4) Assess the stability of the goaf.

Equation (23) is used to calculate the cloud characteristic parameters of the various index evaluation criteria (Tables 1 and 2). Table 11 displays the results. The evaluation level cloud diagram is created using MATLAB software, as illustrated in Figure 10.

In this paper, AHP of Group Decision Theory Cloud Model (AHPGDT-CM), CRITIC-Cloud Model (CRITIC –CM), and Combination Weighting based on Game Theory-Cloud Model (CWGT-CM) are used to calculate the stability of 151 goafs in Duimenshan mine section. According to Equation (24), the comprehensive certainty of the stability of each goaf is calculated, and the stability grade of goaf is determined according to the principle of maximum membership degree. The results are shown in Table 12. The distribution of four stability levels in the goaf is shown in Figure 11.

According to Figure 11, it can be concluded that most of the goafs in the Duimenshan mine section are stable (IV) and relatively stable (III), and only a small number of goafs are in a state of poor stability (II).

3.3. FLAC3D Numerical Simulation

(1) Determining the mechanical parameters of the surrounding rock.

The rocks in and around the Duimenshan section consist mainly of dolomite and siltstone, as indicated by the ground survey. In the FLAC3D model, there are two groups of material parameters required—material deformation parameters, including bulk modulus K and shear modulus G, and material strength parameters, including cohesion C and internal friction angle φ. Additionally, density ρ and gravitational acceleration g of the model material must also be taken into account. The strength parameters of the rock mass utilized in this simulation were chosen based on the findings of rock mechanics tests, which can be found in Table 13.

The model was built using the FLAC3D software, based on the actual size and location of the goaf obtained from the site survey. The model is oriented with the X direction being vertical to the ore body direction, with a length of 3,500 m. The Y direction follows the direction of the ore body and has a length of 4,000 m. The vertical Z direction of the model has

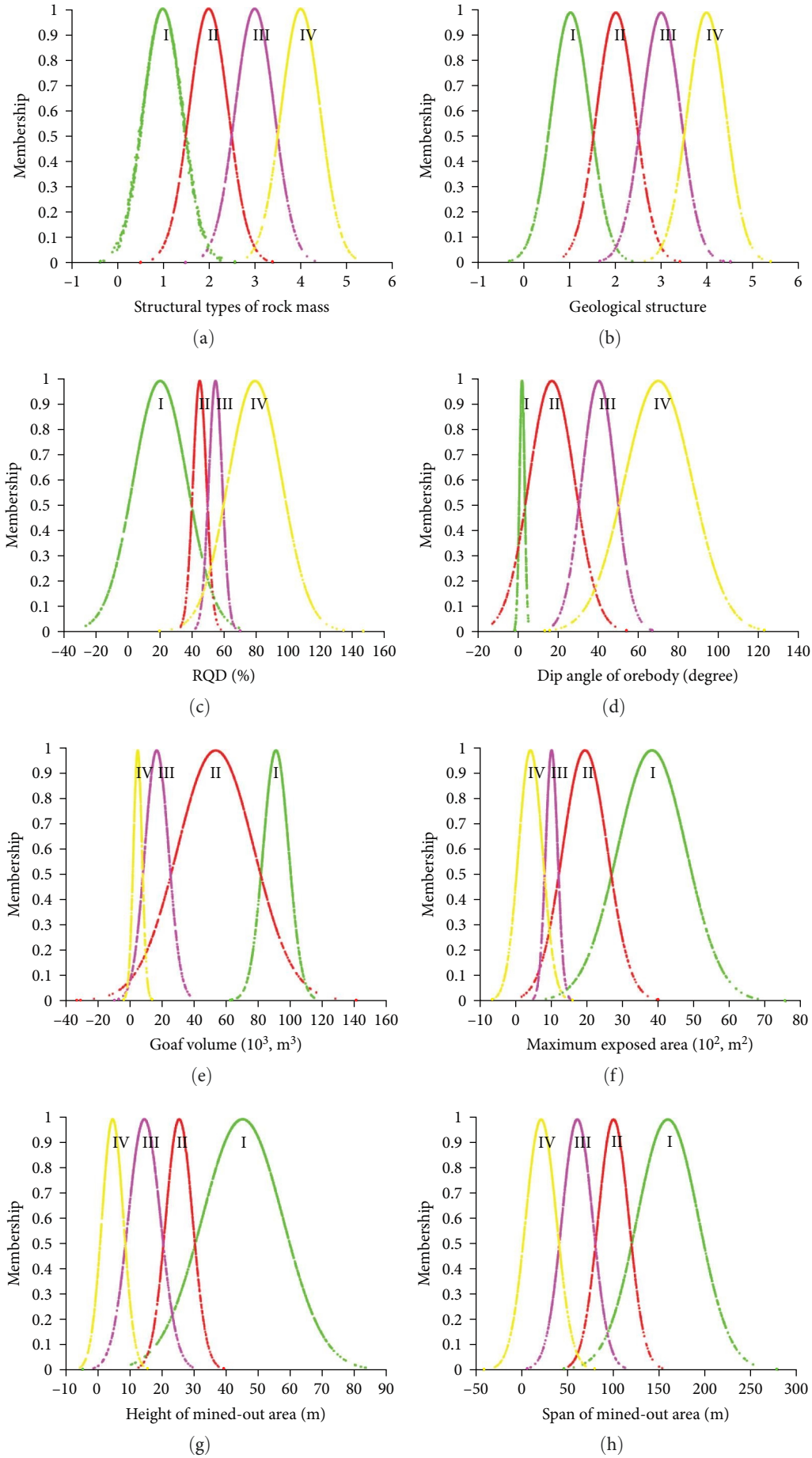

Figure 10: Continued.

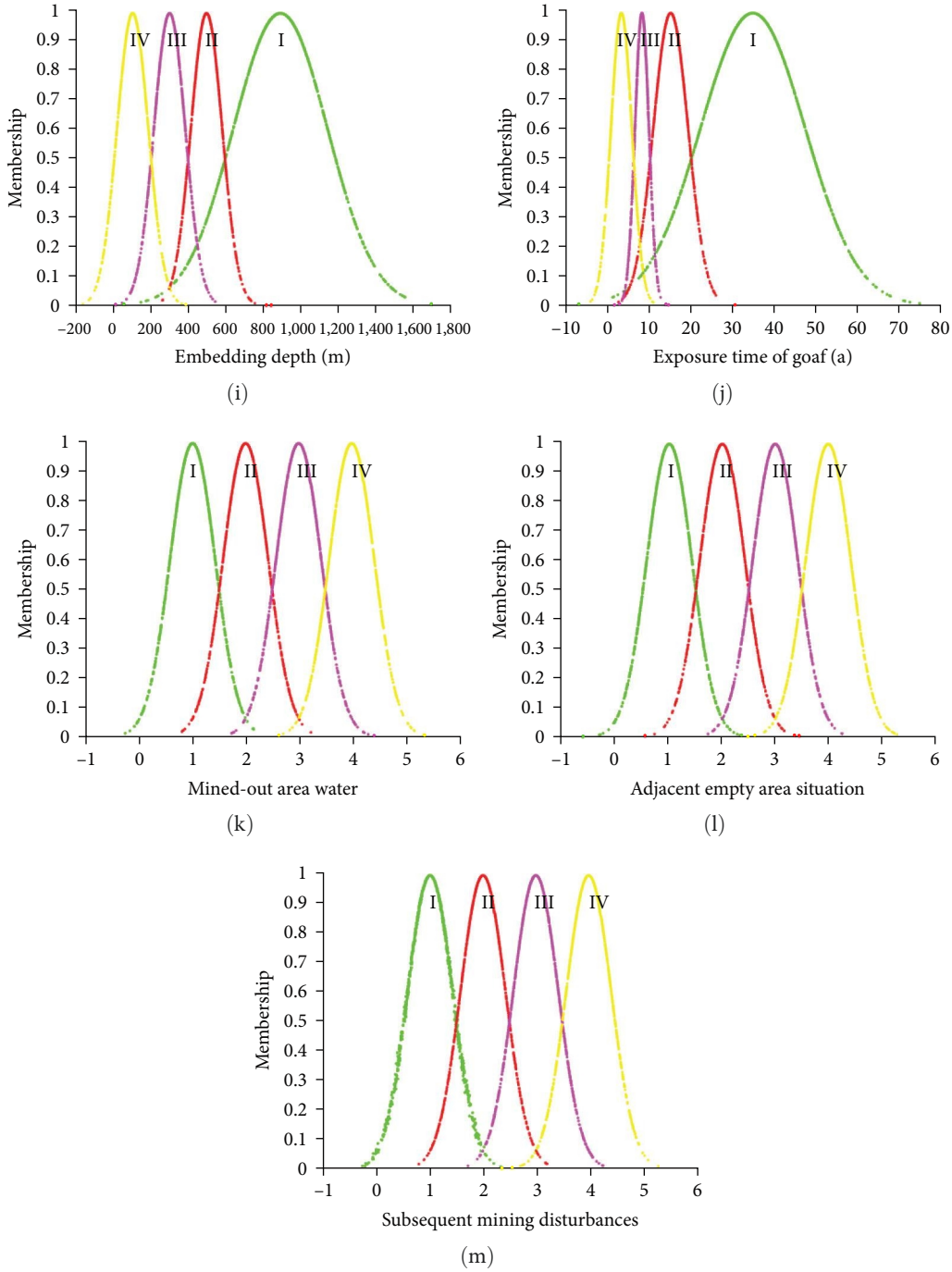

Figure 10: Cloud chart of evaluation levels of different indicators: (a) structural types of rock mass X1, (b) geological structure X2, (c) rock mass quality X3, (d) dip angle of ore body X4, (e) goaf volume X5, (f) maximum exposed area X6, (g) height X7, (h) span of mined-out area X8, (i) embedding depth X9, (j) exposure time of goaf X10, (k) mined-out area water X11, (l) adjacent empty area situation X12, and (m) subsequent mining disturbances X13.

a bottom elevation of 900 m and the top elevation simulates the actual terrain of the mine. Due to the complex terrain, some simplifications were made. The generated model consists of a total of 3,910,425 units and 3,154,125 nodes, as shown in Figures 12 and 13.

The mining process excavates the goaf from top to bottom. This allows for quantitative calculations and analysis of the stress, displacement, and plastic zone distribution of ore and rock in the goaf. Additionally, it facilitates the ability to assess the stability of the goaf. Figure 14 displays the calculation cloud map of 151 goafs.

The calculated cloud map indicates that the roof settlement value of each goaf in Duimenshan mine section ranges from 0.1 to 12.1 cm, with compressive stress values ranging

Table 12: Evaluation results.

No.	Membership of CWGT-CM model				Evaluation level		
					CWGT-CM	AHPGDT-CM	CRITIC-CM
1525-1	0.0418	0.1320	0.1884	0.6440	IV	IV	IV
1525-2	0.0498	0.2451	0.2082	0.5273	IV	IV	IV
1525-3	0.0403	0.1252	0.1570	0.6630	IV	IV	IV
1525-4	0.0497	0.1593	0.5965	0.2754	III	III	III
⋮	⋮	⋮	⋮	⋮	⋮	⋮	⋮
1660-4	0.0263	0.0826	0.1656	0.6760	IV	IV	IV
1660-5	0.0277	0.0981	0.1698	0.6748	IV	IV	IV
1660-6	0.0312	0.1047	0.1089	0.7388	IV	IV	IV
⋮	⋮	⋮	⋮	⋮	⋮	⋮	⋮
1830-3	0.0426	0.3066	0.5757	0.1500	III	III	III
1830-4	0.0422	0.3222	0.5029	0.1936	III	III	III

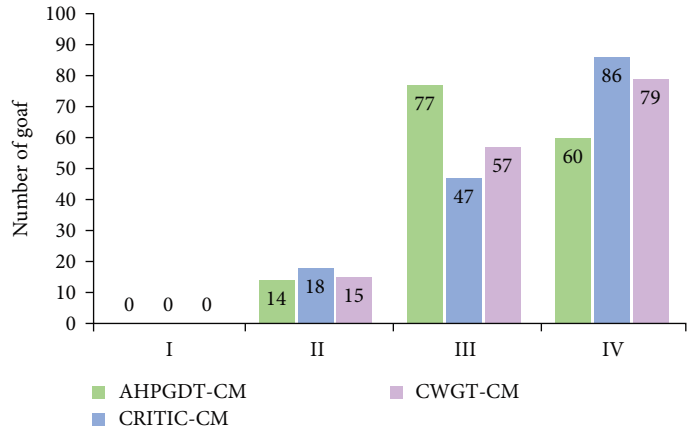

Figure 11: The distribution map of the stability grade of the goaf in the Duimenshan mine section.

Table 13: Macroscopic physical and mechanical parameters of the ore body in the Duimenshan section.

Petrography character	ρ (g/cm^3)	Strength of extension (MPa)	Modulus of elasticity (GPa)	Cohesive force (MPa)	φ (degree)	Poisson's ratio
Siltstone	2.62	0.38	3.55	0.33	33.81	0.24
Dolomite	2.79	0.90	6.87	0.80	35.65	0.19
Limestone	2.64	0.86	6.76	0.77	37.03	0.19
Ore body	2.84	1.11	10.33	1.08	35.97	0.21

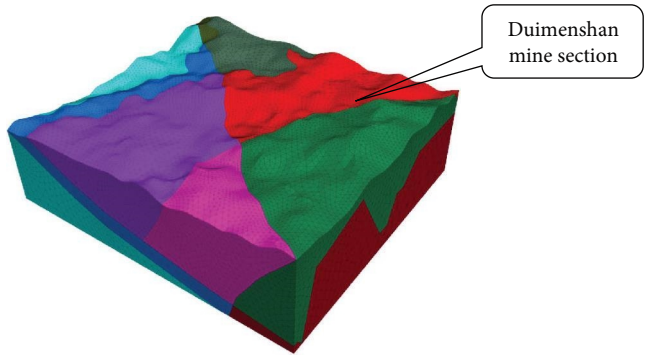

Figure 12: Schematic diagram of the overall 3D model.

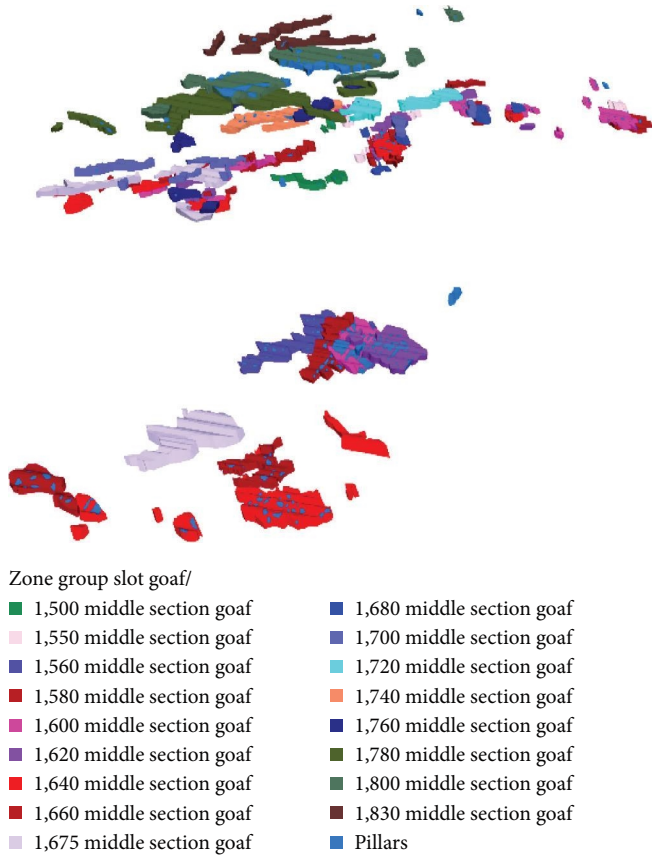

Figure 13: The mined-out area of Duimenshan section.

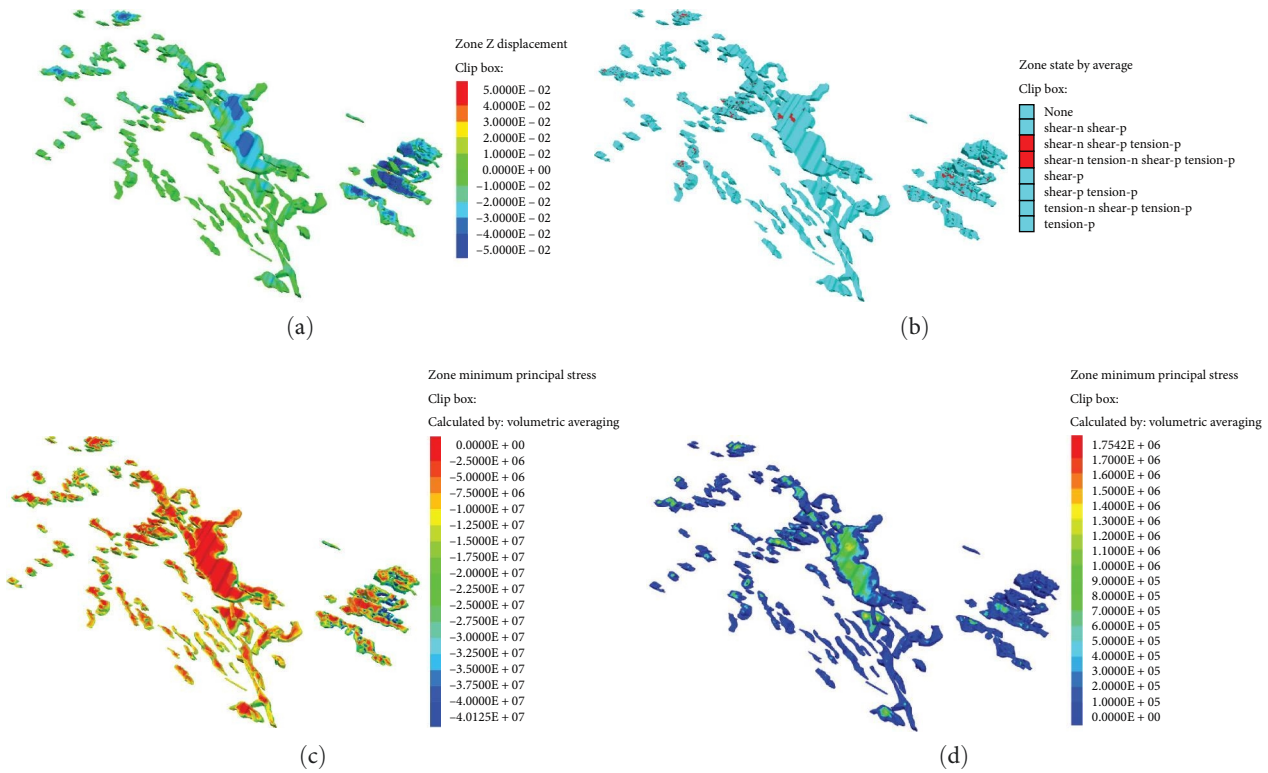

Figure 14: Numerical simulation results of Duimenshan section. (a) Displacement cloud map of each empty area. (b) Cloud map of plastic zone distribution in each empty area. (c) Compressive stress cloud in each empty area. (d) Tensile stress cloud in each empty area.

Table 14: Statistics of numerical simulation calculation of the stability of the goaf.

Number of goaf	Settlement of roof slab (cm)	Top plate tensile stress (Mpa)	Plastic zone distribution	Stability description
1525-1	2.76	0	Almost nothing	IV
1525-2	2.46	0	Almost nothing	IV
1525-3	2.57	0	Almost nothing	IV
1525-4	2.78	0.22	Small distribution	III
⋮	⋮	⋮	⋮	⋮
1640-4	3.78	0.67	Large distribution area	II
1640-5	1.35	0	Almost nothing	IV
1640-6	1.26	0	Almost nothing	IV
⋮	⋮	⋮	⋮	⋮
1830-3	1.67	0	Small distribution	III
1830-4	1.54	0	Small distribution	III

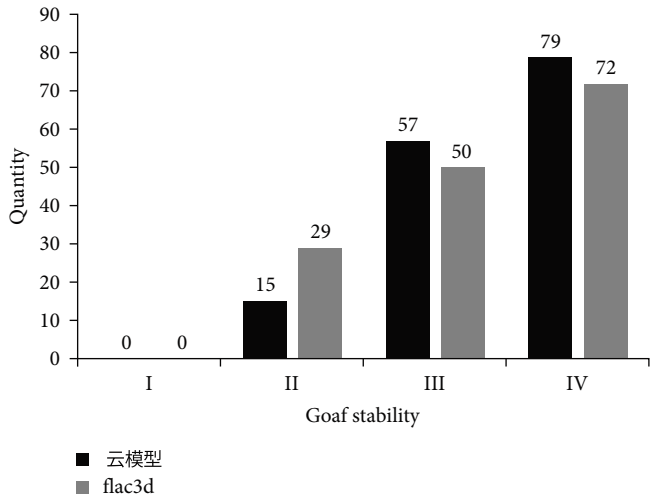

Figure 15: The number of goafs with different stability grades by two methods.

Table 15: Confusion matrix.

FLAC3D	Cloud model evaluation method based on combination assignment				
	I	II	III	IV	总数
I	0	0	0	0	0
II	0	15 (TP)	6 (FN)	8 (FN)	29
III	0	0	50 (TP)	0 (FN)	50
IV	0	0	1 (FN)	71 (TP)	72
Total	0	15	57	79	151

from 16 to 100 MPa and tensile stress values ranging from 0 to 1.75 MPa. The plastic zone in the goaf is dispersed. Table 14 shows the stability statistics of each goaf.

3.4. Comparison of Results. This paper analyzes the stability grade of 151 goafs Duimenshan mine section using the stability grade evaluation method of goaf based on combined weighting cloud model. The stability of these goafs is simulated using FLAC3D software. The comparison of the number of goafs with different stability levels in the two methods is shown in Figure 15. The confusion matrix (Table 15) is constructed using the calculation results of both methods, and the consistency of these results (Equation (25)) is used to validate the feasibility and rationality of the evaluation model:

$$\text{Precision} = \frac{\sum_{i=1}^{4} \text{TP}_i}{\sum_{i=1}^{4} \text{TP}_i + \text{FP}_i}. \tag{25}$$

Using 151 sets of goaf data to compare the consistency of CWGT-CM, AHPGDT-CM, and CRITIC-CM model and

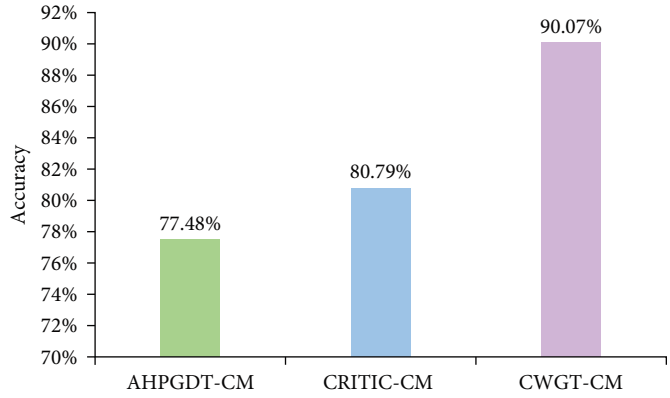

Figure 16: Comparison of evaluation accuracy of three models.

FLAC3D simulation calculation results, and then judge the accuracy of the model. The comparison results are shown in Figure 16.

The evaluation accuracy of AHPGDT-CM model is 77.48%, the evaluation accuracy of CRITIC-CM model is 80.79%, and the evaluation accuracy of CWGT-CM model is 90.07%. It shows that the core of goaf stability evaluation based on cloud model is the determination of index weight, and the accuracy of index weight calculation directly affects the final goaf stability evaluation results. At the same time, it shows that the combination weighting method of goaf stability index weight based on game theory effectively reduces the influence of human subjectivity in AHP but retains the objectivity of CRITIC method. The CWGT-CM model improves the practicability.

4. Conclusions

A cloud model based on combination weighting is proposed to evaluate the stability of goaf in underground mines comprehensively. This is done to reduce the subjectivity of evaluation and consider the fuzziness and randomness of evaluation indexes in the process.

(1) The singleness of weight determination is targeted in this section. First, the subjective weight calculation method of multiple decision makers is proposed, based on group decision theory. This can reflect not only the group of multiple decision makers but also their individuality, thereby improving the rationality of subjective weight. Then, the CRITIC objective weight calculation method is proposed, which considers the index conflict and contrast strength comprehensively. Additionally, the influence of different dimensionless methods on the calculation results of the CRITIC method is compared. The differentiated range transformation method (MMS-NMMS) is concluded to be the most suitable dimensionless method. This method can fully consider the index conflict and contrast strength, thereby improving the scientific nature of objective weight. The weights are combined using game theory, which finds a balance between subjective and objective weights to obtain the optimal comprehensive weight. This increases the accuracy of the evaluation results.

(2) The cloud model has a strong universality and can convert abstract qualitative concepts into specific quantitative values. It has a positive effect on the randomness and fuzziness of the stability classification of the goaf, improving the accuracy of the evaluation results.

(3) Using 151 sets of goaf data to compare the consistency of CWGT-CM, AHPGDT-CM, and CRITIC-CM model and FLAC3D simulation calculation results, and then judge the accuracy of the model. It shows that the core of goaf stability evaluation based on cloud model is the determination of index weight, and the accuracy of index weight calculation directly affects the final goaf stability evaluation results. At the same time, it shows that the combination weighting method of goaf stability index weight based on game theory effectively reduces the influence of human subjectivity in AHP, but retains the objectivity of CRITIC method. Improve the practicability.

(4) The method was applied to 151 underground goafs in the Duimenshan mine section, significantly improving the calculation efficiency. The evaluation results were compared with the numerical simulation results from FLAC3D, resulting in a 90% consistency rate.

Data Availability

The data used to support the findings of this study are included in this article.

Conflicts of Interest

The authors declare that they have no conflicts of interest.

Supplementary Materials

Table S1: judgment matrix of decision maker D1. Table S2: judgment matrix of decision maker D2. Table S3: judgment matrix of decision maker D3. Table S4: judgment matrix of decision maker D4. Table S5: judgment matrix of decision

maker D5. Table S6: judgment matrix of decision maker D6. Table S7: judgment matrix of decision maker D7. Table S8: judgment matrix of decision maker D8. Table S9: judgment matrix of decision maker D9. Table S10: judgment matrix of decision maker D10. (*Supplementary Materials*)

References

[1] Ministry of Emergency Management of the People's Republic of China, "2017 National statistical analysis report on production and safety accidents in non-coal mines released," *Occupational Health and Emergency Rescue*, vol. 36, no. 3, Article ID 284, 2018.

[2] Y. Shang, Y. Guo, and W. Zhang, "Numerical simulation on the deformation and failure of the goaf surrounding rock in Heiwang mine," *IOP Conference Series: Earth and Environmental Science*, vol. 121, Article ID 052034, 2018.

[3] D. F. Liu, C. W. Liu, F. Zhang, Y. Liu, and B. B. Guo, "Research on the construction and application of microseismic monitoring system based on stress analysis," *Journal of Mining and Safety Engineering*, vol. 33, no. 5, pp. 932–937, 2016.

[4] N. Jia, W. Chao, Z. Q. Luo, and C. Y. Xie, "Comprehensive identification of stability of air-mining zones with ITOPSIS coupled with PSF," *Journal of Northeastern University (Natural Science Edition)*, vol. 37, no. 8, pp. 1182–1187, 2016.

[5] K. Zhao, M. F. Cai, Y. Z. Rao, J. Rao, and J. X. Zhu, "A fuzzy stochastic reliability study of block stability in a quarrying zone," *Geotechnics*, no. 6, pp. 987–990, 2003.

[6] J. Hu, X. C. Zhang, K. P. Zhou, X. H. Du, and T. Lei, "Empty zone stability identification based on D-S evidence theory with engineering applications," *Journal of Chongqing University*, vol. 36, no. 9, pp. 35–42, 2013.

[7] R. He, H. Liu, F. Ren, G. Li, J. Zhang, and Y. Zhou, "Comprehensive evaluation and decision for goaf based on fuzzy theory in underground metal mine," *Advances in Civil Engineering*, vol. 2022, Article ID 3104961, 14 pages, 2022.

[8] Y. Qin, Z. Luo, J. Wang, S. Ma, and C. Feng, "Evaluation of goaf stability based on transfer learning theory of artificial intelligence," *IEEE Access*, vol. 7, pp. 96912–96925, 2019.

[9] L. Wang, Q. Guo, J. Luo, Y. Zhang, Z. Wan, and X. Wang, "A novel evaluation method for the stability of construction sites on an abandoned goaf: a case study," *KSCE Journal of Civil Engineering*, vol. 26, no. 6, pp. 2835–2845, 2022.

[10] S. Luo, W. Liang, G. Zhao, and J. Wang, "Evaluation of point-pillar stability using a hesitant fuzzy GA-WDBA approach," *International Journal of Fuzzy Systems*, vol. 24, pp. 3702–3714, 2022.

[11] H. Yuan, Z. Cao, L. Xiong, H. Li, and Y. Wang, "A machine learning method for engineering risk identification of goaf," *Water*, vol. 14, no. 24, Article ID 4075, 2022.

[12] W. R. Lian, N. Hao, Z. L. Dun, E. Liu, and W. F. Yang, "High-speed railroad foundation "activation" grading method in hollow area and engineering application," *Geotechnical Mechanics*, vol. 43, no. S2, pp. 401–413, 2022.

[13] L. Liu and Z. Q. Chen, "Application of fuzzy set-pair analysis in the stability evaluation of mining airspace," *Journal of South Central University (Natural Science Edition)*, vol. 46, no. 7, pp. 2665–2672, 2015.

[14] Y. Feng, X. Wang, X. Min, A. B. Cheng, Q. L. Zhang, and J. W. Zhao, "Optimization of hazard evaluation method for mining airspace," *Journal of South Central University (Natural Science Edition)*, vol. 44, no. 7, pp. 2881–2888, 2013.

[15] H. J. Hu, D. Nguyen, K. P. Chou, and N. Yang, "Environmental safety identification and synergistic utilization of residual mining operation based on the structural effect of empty zone," *Journal of South Central University (Natural Science Edition)*, vol. 44, no. 3, pp. 1122–1130, 2013.

[16] N. Wang, Z. Zhong, X. Liu, and G. Gao, "Failure mechanism of anti-inclined karst slope induced by underground multiseam mining," *Geofluids*, vol. 2022, Article ID 1302861, 13 pages, 2022.

[17] B. Luo, Y. Ye, N. Yao, and Q. Wang, "Interval number ranking method based on multiple decision attitudes and its application in decision making," *Soft Computing*, vol. 25, no. 5, pp. 4091–4101, 2021.

[18] N. Yao, Y. Ye, Q. Wang, and N. Hu, "Interval number ranking method considering multiple decision attitudes," *Iranian Journal of Fuzzy Systems*, vol. 17, no. 2, pp. 115–127, 2020.

[19] L. Wang, Q. Guo, and X. Yu, "Stability-level evaluation of the construction site above the goaf based on combination weighting and cloud model," *Sustainability*, vol. 15, no. 9, 2023.

[20] J. Chen, Y. Wang, S. Zhu, and Y. Xie, "Application of the cloud model synthesis method in ecological evaluation of waterways," *Mathematical Problems in Engineering*, vol. 2022, Article ID 9382277, 11 pages, 2022.

[21] M. J. Dobrow, V. Hagens, R. Chafe, T. Sullivan, and L. Rabeneck, "Consolidated principles for screening based on a systematic review and consensus process," *Canadian Medical Association Journal*, vol. 190, no. 14, pp. E422–E429, 2018.

[22] Y. Ye, N. Yao, Q. Wang, and Q. Wang, "A method of ranking interval numbers based on degrees for multiple attribute decision making," *Journal of Intelligent & Fuzzy Systems*, vol. 30, no. 1, pp. 211–221, 2016.

[23] D. Kyne, "Storm surge risk assessment in coastal communities in the Rio Grande Valley: an application of GIS-based spatial multicriteria decision analysis with analytical hierarchy process," *Journal of Coastal Research*, vol. 39, no. 3, 2023.

[24] A. Kumar and S. Pant, "Analytical hierarchy process for sustainable agriculture: an overview," *MethodsX*, vol. 10, Article ID 101954, 2023.

[25] X. Peng, H. Xinli, W. Shuangshuang, Y. Chunye, and L. Chang, "Slope stability analysis based on group decision theory and fuzzy comprehensive evaluation," *Journal of Earth Science*, vol. 31, pp. 1121–1132, 2020.

[26] M. Collan, M. Fedrizzi, and P. Luukka, "Possibilistic risk aversion in group decisions: theory with application in the insurance of giga-investments valued through the fuzzy pay-off method," *Soft Computing*, vol. 21, no. 15, pp. 4375–4386, 2017.

[27] J. C. Bezdek, B. Spillman, and R. Spillman, "Fuzzy relation spaces for group decision theory: an application," *Fuzzy Sets and Systems*, vol. 2, no. 1, pp. 5–14, 1979.

[28] S. Zhong, Y. Chen, and Y. Miao, "Using improved CRITIC method to evaluate thermal coal suppliers," *Scientific Reports*, vol. 13, Article ID 195, 2023.

[29] Z. Shanshan, W. Guiwu, L. Rui, and C. Xudong, "Cumulative prospect theory integrated CRITIC and TOPSIS methods for intuitionistic fuzzy multiple attribute group decision making," *Journal of Intelligent & Fuzzy Systems*, vol. 43, no. 6, pp. 7793–7806, 2022.

[30] R. Tian and J. Wu, "Groundwater quality appraisal by improved set pair analysis with game theory weightage and health risk estimation of contaminants for Xuecha drinking water source in a loess area in Northwest China," *Human and Ecological Risk Assessment: An International Journal*, vol. 25, no. 1-2, pp. 132–157, 2019.

[31] X. Wang, G. Wang, Y. Wu, Y. Xu, and H. Gao, "Comprehensive assessment of regional water usage efficiency control based on game theory weight and a matter-element model," *Water*, vol. 9, no. 2, Article ID 113, 2017.

[32] Q. Wu, A. Qi, and G. Zhao, "Evaluation of energy utilisation efficiency of central air conditioning in large buildings based on entropy weight-cloud model," *International Journal of Global Energy Issues*, vol. 44, no. 2-3, pp. 198–216, 2022.

[33] Z. Meng, Z. Yi, J. Li, X. Wang, and Z. Wang, "Evaluation of cloud model for public transport service quality," *IOP Conference Series: Materials Science and Engineering*, vol. 688, Article ID 022019, 2019.

[34] D. L. Wang and R. W. Dai, "A study of convergence of expert groupthink," *Journal of Management Science*, no. 2, pp. 1–5, 2002.